

PERIODICO di MINERALOGIA  
established in 1930

*An International Journal of  
MINERALOGY, CRYSTALLOGRAPHY, GEOCHEMISTRY,  
ORE DEPOSITS, PETROLOGY, VOLCANOLOGY*  
and applied topics on *Environment, Archeometry and Cultural Heritage*

*Special Issue in memory of Sergio Lucchesi*

## First occurrence of titanomagnetites from the websterite dykes within Balmuccia peridotite (Ivrea-Verbano zone): crystal chemistry and structural refinement

Davide Lenaz\* and Francesco Princivalle

Dipartimento di Geoscienze, Università di Trieste, Italy

\*Corresponding author: [lenaz@units.it](mailto:lenaz@units.it)

### Abstract

The crystal chemistry of three ulvöspinel from the websteritic dykes within the Balmuccia peridotites has been investigated by means of X-ray single crystal diffraction and electron microprobe. They are very similar each other with cell edge about 8.43 Å and oxygen positional parameter between 0.2565 and 0.2570. Ti content is about 0.32 a.p.f.u. As they are embedded in a glass with syenite composition it is supposed they quenched during the rapid cooling of a melt pervading the websteritic dykes. This is the first finding of similar spinels in the studied area.

*Key words:* Balmuccia peridotite; websterite dykes; ulvöspinel; crystal chemistry; structural refinement.

### Introduction

Minerals in the solid solution series between magnetite (Fe<sub>3</sub>O<sub>4</sub>) and ulvöspinel (Fe<sub>2</sub>TiO<sub>4</sub>) are common constituent of a wide variety of igneous and metamorphic rocks. Intermediate members of the series are the primary carriers of rock magnetism. The magnetic properties of these materials are critically dependent upon their composition, degree of oxidation and intracrystalline cation distribution. Magnetite-Ulvöspinel solid solutions [(1-x)Fe<sub>3</sub>O<sub>4</sub> - x(Fe<sub>2</sub>TiO<sub>4</sub>)] have the inverse spinel structure. Variations of the unit-cell parameter, a<sub>0</sub>, with

composition for synthetic solid solutions have been presented by Lindsley (1965). The relation is linear in the range 20-80 mole per cent Fe<sub>2</sub>TiO<sub>4</sub>. Changes in slope appear below 20 and above 80 mole per cent. As concerns the oxygen positional parameter, *u*, Syono (1965) reported that neutron diffraction measurements gave  $u = 0.261 \pm 0.001$  for  $x = 0.99$  and  $u = 0.255 \pm 0.001$  for  $x = 0.56$ . Studies on natural titanomagnetites are fairly rare (Stout and Bayliss, 1975; 1980). A systematic study of the crystal structure of synthetic powder specimens of titanomagnetites in order to characterize the effects of composition and quenching temperature on the

cation distribution was undertaken by Wechsler et al. (1984). Fujino (1974) studied the variation of structural parameter for different composition of synthetic titanomagnetites along the join  $\text{Fe}_3\text{O}_4\text{-Fe}_2\text{TiO}_4$ . Recently, Bosi et al. (2009) synthesized 19 spinels along the magnetite-ulvöspinel series by using a flux-growth method. The unit-cell parameter, oxygen fractional coordinate, and tetrahedral bond length increase with increasing ulvöspinel component, whereas the octahedral bond length decreases marginally.

During a field trip in Balmuccia, websterite dykes and lherzolite were sampled in order to study the differences in crystal-chemistry of Cr-spinels. In the websterite dykes two types of spinels were found, very small Cr-spinels with low Cr-amount that are not suitable for diffraction studies and some larger titanomagnetite spinels. To our knowledge, this is the first occurrence of this kind of spinels in Balmuccia and one of the few crystalchemical studies on natural ulvöspinel.

### Geological setting

The Ivrea-Verbano zone (Italian Western Alps) is considered to be a section of the deep crust (Mehnert, 1975). It can be divided into three main units: a) basal mantle tectonites (Baldissero, Balmuccia and Finero occurrences); b) overlying layered series, probably related to various mafic intrusive cycles, near the mantle-crust boundary; c) kinzigitic series at the top of the complex. The Balmuccia peridotite is an elongate body parallel to the Insubric Line, and is exposed over some 4 km<sup>2</sup>. It is cut by a remarkable dyke network. In the Balmuccia tectonite the main lithotypes are lherzolites and dunites, harzburgites is rare. In the lherzolite, spinel is variable in composition, with Cr-number  $[100 \times \text{Cr}/(\text{Cr}+\text{Al})]$  of 10 - 25 in normal lherzolites and 3 - 12 in lherzolite adjacent to Al-augite pyroxenite (Comin-Chiaramonti et al., 1982; Mukasa and Shervais, 1999). The peridotite is characterised by a dyke network, most dykes of which are concordant or

subconcordant with the main foliation. Shervais (1979a, b) classified them into two main types, a Cr-diopside series and an Al-augite series, based on pyroxene chemistry. The dykes of Cr-diopside series (older dykes) comprise clinopyroxenites, websterites ( $\pm$  olivine) and bronzitites with rare Cr-bearing spinel and amphibole (Sinigoj et al., 1983; Mukasa and Shervais, 1999). At least three generations of dykes can be demonstrated based on crosscutting relationships. Cr-spinels show Cr-number in the range 5-22 (Comin-Chiaramonti et al., 1982; Mukasa and Shervais, 1999). The dykes of the Al-augite series are spinel-rich websterites with rare amphibole and comprise various types of dykes characterised by a high modal content of Al-spinel (Cr-number  $< 1 - 4$ ). These websterites are younger than the Cr-diopside suite. Cr-bearing spinels from the Al-augite dykes and the lherzolite body have been described by Basso et al. (1984) and Princivalle et al. (1989). Recently, Lenaz et al. (2005) described the occurrences of Mg-chromitites dykes within the peridotite body. According to Sinigoj et al. (1983) the Balmuccia peridotite shows evidence, in the form of a network of dykes, of partial melting and flow crystallization processes. The mineral assemblages of the peridotite and websterite are re-equilibrated at 800-900 °C (in Rivalenti et al., 1995).

### Experimental procedures, structural and chemical data

Three single crystals of titanomagnetites from a Cr-diopside dyke were analysed. One of them shows a large apatite inclusion inside, the others are bordered by a glassy-like mesostasis with syenitic composition. X-ray diffraction data were recorded on an automated KUMA-KM4 (K-geometry) diffractometer, using  $\text{MoK}\alpha$  radiation, monochromatised by a flat graphite crystal, at the University of Trieste (Italy). Data collection was made, according to Della Giusta et al. (1996), up

to  $55^\circ$  of  $2\theta$  in the  $\omega$ - $2\theta$  scan mode, scan width  $1.8^\circ 2\theta$ , counting time 20-50 seconds. Twenty-four equivalent reflections of (12 8 4) peak, at about  $80^\circ$  of  $2\theta$ , were accurately centred at both sides of  $2\theta$ , and the  $\alpha_1$  peak baricentre was used for cell parameter determination. Corrections for absorption were performed according to North et al. (1968). Structural refinement using the SHELX-97 program (Sheldrick, 1997) was carried out against  $Fo^2_{hkl}$  in the  $Fd-3m$  space group (with origin at  $\bar{3}m$ ), since no evidence of different symmetry appeared. Refined parameters were scale factor, oxygen positional parameter ( $u$ ), tetrahedral and octahedral site occupancies, and thermal displacement parameter ( $U_{eq}$ ). Scattering factors were taken from Tokonami (1965) and Prince (2004). No constraints were imposed by chemical analyses. Crystallographic data are listed in Table 1.

Ten to fifteen spot chemical analyses were performed on the same crystals used for X-ray data collection using a CAMECA SX50 electron microprobe operating at 15 kV and 15 nA, 10 s counting time for peak and 5 sec for total background. Synthetic oxide standards (MgO, FeO, MnO, ZnO, NiO,  $Al_2O_3$ ,  $Cr_2O_3$ ,  $TiO_2$  and  $SiO_2$ ) were used. The raw data were reduced with PAP-type correction software provided by CAMECA.

Results are considered accurate between 2-3% for major elements and within 10% for minor elements. Iron oxide was calculated totally as ferrous oxide; ferric iron was recalculated by stoichiometry. Cation distribution (Table 1) between T and M sites were obtained with the method described by Lavina et al. (2002), in which crystal chemical parameters are calculated as a function of the atomic fractions at the two sites and fitted to the observed ones. Site atomic fractions are calculated by minimising the function  $F(X)$  which takes into account the mean of the square differences between calculated and observed parameters, divided by their square standard deviations (Table 1).

Table 1. Structural parameters, refinement details, chemical analyses and cation distribution.

|              | BAL-USP   | BAL-USP1   | BAL-USP2  |
|--------------|-----------|------------|-----------|
| $a_0$        | 8.4306(2) | 8.4310(2)  | 8.4305(2) |
| $u$          | 0.2565(1) | 0.25665(9) | 8.2570(1) |
| m.a.n.T      | 25.5 (5)  | 25.6 (3)   | 25.6 (4)  |
| m.a.n.M      | 24.2 (2)  | 24.1 (1)   | 24.0 (3)  |
| T-O          | 1.920 (1) | 1.922 (1)  | 1.927 (1) |
| M-O          | 2.054 (1) | 2.053 (1)  | 2.050 (1) |
| $N_{refl}$   | 151       | 146        | 137       |
| $U_{eq}$ (T) | 701(10)   | 645(10)    | 674(15)   |
| $U_{eq}$ (M) | 740(8)    | 667(7)     | 700(10)   |
| $U_{eq}$ (O) | 1005(22)  | 954(18)    | 1011(27)  |
| R1           | 1.76      | 1.51       | 2.11      |
| wR2          | 3.17      | 2.54       | 3.17      |
| Goof         | 1.122     | 1.122      | 1.118     |
| MgO          | 2.26 (8)  | 2.29(11)   | 2.25(7)   |
| $Al_2O_3$    | 2.03 (7)  | 2.01(4)    | 2.03(4)   |
| $SiO_2$      | 0.21(4)   | 0.20(3)    | 0.26(3)   |
| $TiO_2$      | 11.85(16) | 11.86(12)  | 11.72(17) |
| MnO          | 1.57(5)   | 1.61(8)    | 1.55(12)  |
| $FeO_{tot}$  | 78.14(60) | 77.96(56)  | 78.05(57) |
| Sum          | 96.06     | 95.93      | 95.86     |
| FeO          | 37.79(42) | 37.66(40)  | 37.71(40) |
| $Fe_2O_3$    | 44.84(46) | 44.78(42)  | 44.83(43) |
| Sum          | 100.55    | 100.42     | 100.35    |
| T site       |           |            |           |
| Mg           | 0.048(5)  | 0.018(3)   | 0.061(3)  |
| Al           | 0.000(0)  | 0.000(0)   | 0.000(0)  |
| Si           | 0.007(2)  | 0.007(1)   | 0.009(1)  |
| Mn           | 0.049(3)  | 0.051(3)   | 0.050(4)  |
| $Fe^{2+}$    | 0.227(4)  | 0.259(4)   | 0.263(4)  |
| $Fe^{3+}$    | 0.669(7)  | 0.665(7)   | 0.617(7)  |
| $\Sigma$     | 1.000     | 1.000      | 1.000     |
| M site       |           |            |           |
| Mg           | 0.075(5)  | 0.108(5)   | 0.064(3)  |
| Al           | 0.088(6)  | 0.087(5)   | 0.088(4)  |
| Ti           | 0.328(11) | 0.329(9)   | 0.325(8)  |
| $Fe^{2+}$    | 0.936(19) | 0.902(15)  | 0.900(13) |
| $Fe^{3+}$    | 0.573(15) | 0.574(12)  | 0.623(11) |
| $\Sigma$     | 2.000     | 2.000      | 2.000     |
| F(x)         | 0.091     | 0.115      | 0.419     |

$a_0$ : unit cell parameter ( $\text{\AA}$ );  $u$ : oxygen fractional coordinate; m.a.n.T and m.a.n.M: mean atomic number in T and M site, respectively; T-O and M-O: tetrahedral and octahedral bond lengths, respectively;  $U_{eq}$ : displacement parameter ( $\text{\AA}^2$ ); R1 (%) and wR2 (%): disagreement indexes (Sheldrick, 1997); Goof: goodness of fit.  $F(X)$ : minimization factor which takes into account the mean of the square differences between calculated and observed parameters, divided by their square standard deviations (Lavina et al., 2002).

### Discussion and conclusions

Lattice parameters of the here studied spinels are very similar to one another, ranging between 8.4305(2) and 8.4310(2) Å, while oxygen positional parameters  $u$  are comprised within 0.25652(11) and 0.25699(13). As regards chemical analyses, the here studied spinels show Fe<sub>2</sub>O<sub>3</sub> content higher than FeO (about 44.8 wt.% vs. 37.7 wt.%), TiO<sub>2</sub> about 11.8 wt.%, MgO about 2.27 wt.%, Al<sub>2</sub>O<sub>3</sub> about 2.02 wt.%, MnO about 1.58 wt.%. The oxygen positional parameter,  $u$ , vs. the cell edge,  $a_0$ , is represented in Figure 1 where their position within a

quadrilateral field including Fe<sub>3</sub>O<sub>4</sub>, Fe<sub>2</sub>TiO<sub>4</sub>, MgCr<sub>2</sub>O<sub>4</sub> and FeCr<sub>2</sub>O<sub>4</sub> is represented. For comparison, natural (Stout and Bayliss, 1975; 1980) and synthetic ulvöspinel with different ulvöspinel content are plotted (Wechsler et al., 1984; Bosi et al., 2009). MgFe<sub>2</sub>O<sub>4</sub> (Andreozzi et al., 2001), MgCr<sub>2</sub>O<sub>4</sub> and FeCr<sub>2</sub>O<sub>4</sub> (Lenaz et al., 2004) synthetic end-members are also plotted. In Figure 2, where M-O vs. T-O values are plotted, the synthetic magnetite - ulvöspinel series by Fujino (1974) is also reported.

The ferrian ulvöspinel analysed by Stout and Bayliss (1975; 1980) have 59-74 mole % of ulvöspinel component and other oxides are

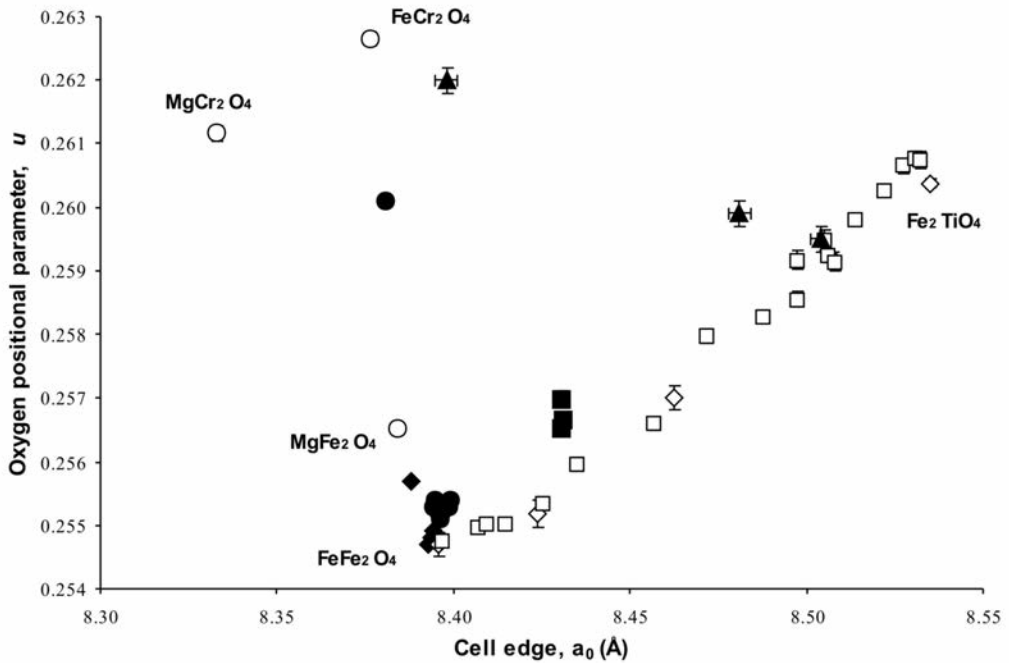


Figure 1. Oxygen positional parameter,  $u$  vs. cell edge,  $a_0$  (Å). Full squares: Balmuccia spinels; full triangles: British Columbia titanomagnetites (Stout and Bayliss, 1975; 1980); full circles: natural magnetites (Della Giusta et al., 1987); open diamonds: synthetic titanomagnetites (Wechsler et al., 1984); open squares: synthetic titanomagnetites (Bosi et al., 2009); open circles: synthetic MgFe<sub>2</sub>O<sub>4</sub> (Andreozzi et al., 2001), synthetic MgCr<sub>2</sub>O<sub>4</sub> (Lenaz et al., 2004), synthetic FeCr<sub>2</sub>O<sub>4</sub> (Lenaz et al., 2006).

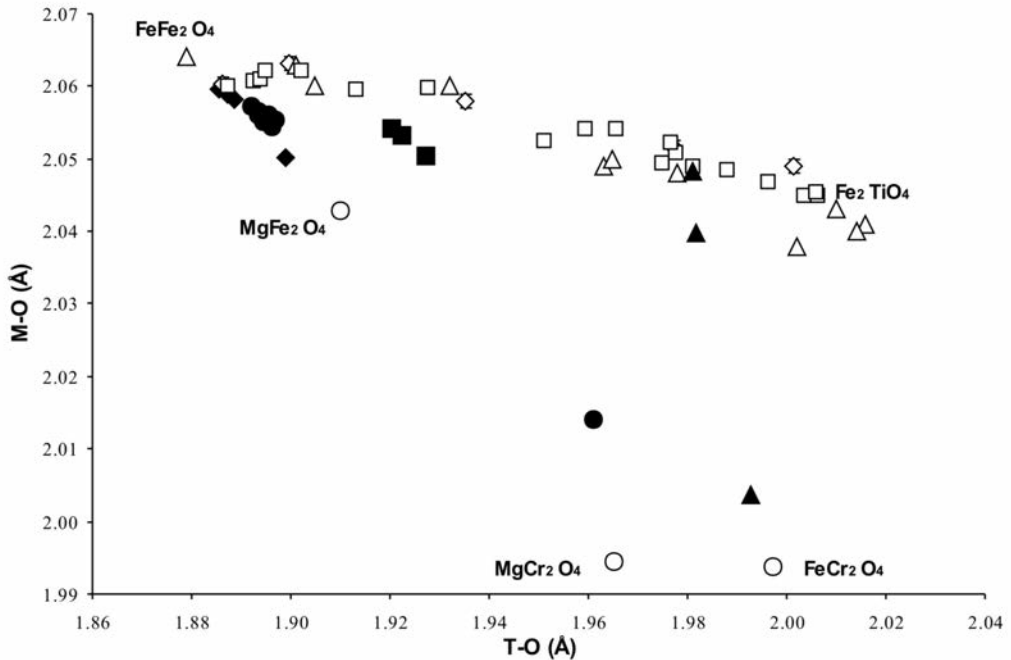


Figure 2. M-O (Å) vs. T-O (Å). Full squares: Balmuccia spinels; full triangles: British Columbia titanomagnetites (Stout and Bayliss, 1975; 1980); full circles: natural magnetites (Della Giusta et al., 1987); open diamonds: synthetic titanomagnetites (Wechsler et al., 1984); open squares: synthetic titanomagnetites (Bosi et al., 2009); open triangles: synthetic titanomagnetites (Fujino, 1974); open circles: synthetic  $\text{MgFe}_2\text{O}_4$  (Andreozzi et al., 2001), synthetic  $\text{MgCr}_2\text{O}_4$  (Lenaz et al., 2004), synthetic  $\text{FeCr}_2\text{O}_4$  (Lenaz et al., 2006).

present in percentages lower than 3%. While the natural so-called ulvöspinel analyzed by Stout and Bayliss (1975; 1980) plot, strangely, far away from the tie line connecting the magnetite and ulvöspinel end-members (and, on the contrary are close to the tie line connecting chromite and ulvöspinel end-members), the here studied spinels are rather close to the synthetic spinels. In particular they are very close to sample FETI20A (Bosi et al., 2009) which present about 35 mole % of ulvöspinel component. The here studied spinels show compositions close to 33 mole % of ulvöspinel component, moving slightly from the “ideal” composition due to the presence of about 6% of

other oxides in the structure ( $\text{MgO}$ ,  $\text{Al}_2\text{O}_3$  and  $\text{MnO}$ ). These data confirm the strong relations between cell edge, oxygen positional parameter and chemical composition in these spinels. Unfortunately, it is unclear why the titanomagnetite analysed by Stout and Bayliss (1975) is so different.

Recently, Pearce et al. (2010) by using X-ray magnetic circular dichroism found out that  $\text{Fe}^{2+}$  only entered the tetrahedral sites when Ti content was  $> 0.40$  atoms per formula units (apfu), whereas  $\text{Fe}^{2+}$  in octahedral sites increased from 1 apfu in magnetite to a maximum of about 1.4 apfu when Ti content was 0.45. These observations are in contrast with those by Bosi et al. (2009), using

unit-cell parameter, chemical composition, and Mössbauer spectroscopy, and Hamdeh et al. (1999) that used peak-area analyses of Mössbauer spectra at 4.2 K to define the distribution regions of  $\text{Fe}^{2+}$  and  $\text{Fe}^{3+}$ , citing only the most recent, where ferroan iron enters the T site also with very low ulvöspinel component. Our study shows how the behaviour of natural samples is quite close to those recorded by Bosi et al. (2009) and Hamdeh et al. (1999) having  $\text{Fe}^{2+}$  in tetrahedral site even with Ti lower than 0.4 apfu and that this result is corroborated by unit cell parameter and the oxygen positional parameter. In fact, it is to notice that by using both Shannon (1976) and Lavina et al. (2002) bond distances we obtain a good agreement for both parameters. By using

Table 2. Chemical analyses of embedding glass.

|                         | GI-USP1  | GI-USP2  |
|-------------------------|----------|----------|
| $\text{Na}_2\text{O}$   | 6.1 (3)  | 6.0 (2)  |
| $\text{MgO}$            | 0.38 (3) | 0.39 (3) |
| $\text{Al}_2\text{O}_3$ | 18.8 (1) | 18.9 (3) |
| $\text{SiO}_2$          | 62.9 (3) | 62.7 (4) |
| $\text{K}_2\text{O}$    | 6.8 (2)  | 6.7 (2)  |
| $\text{CaO}$            | 1.39(5)  | 1.4 (1)  |
| $\text{MnO}$            | 0.20 (7) | 0.14 (7) |
| $\text{FeO}$            | 3.21 (9) | 3.4 (3)  |

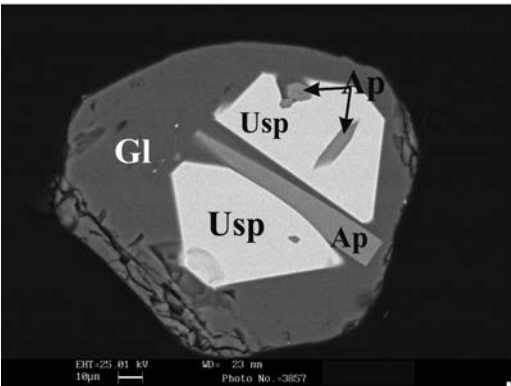
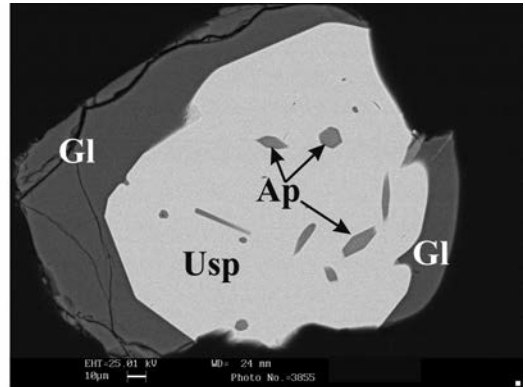
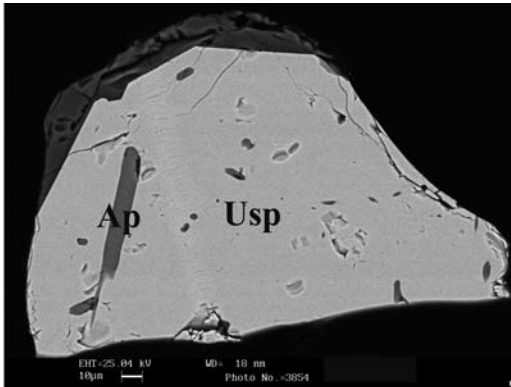


Figure 3. Polished section of analysed titanomagnetites. Above Bal-Usp (left) and Bal-Usp1 (right) crystals, below Bal-Usp2. Usp: ulvöspinel; Ap: apatite; Gl: glass with syenitic composition.

the model of cation distribution suggested by Pearce et al. (2010) with all the ferroan iron in M site, we calculated the parameters of our spinel BAL-USP. What we obtained is a rather different cell edge equal to 8.4409 Å instead of 8.4306 Å and an  $u$  value equal to 0.2541 instead of 0.2565. Obviously, also the T-O and M-O bond lengths are very different. In fact the values calculated with Pearce cation distribution model are 1.887 and 2.076 for T-O and M-O, respectively, while those observed are 1.920 and 2.054.

As already noticed, one of the most remarkable feature of these spinels is that they are embedded in a glass with syenite compositions (Table 2) and that apatite needles are present within them (Figure 3). Probably these ulvöspinel quenched during the rapid cooling of a melt pervading the websteritic dykes.

### Acknowledgements

The Italian C.N.R. financed the installation and maintenance of the microprobe laboratory in Padova. R. Carampin, L. Tauro and L. Furlan are kindly acknowledged for technical support. This work was supported with MURST and Trieste University grants to FP (Studio dello stato di ossidazione e degli elementi in tracce in spinelli a Fe e Cr: implicazioni petrologiche. PRIN 2008). S. Carbonin and F. Nestola are kindly acknowledged for their suggestions that improved the quality of the paper.

### References

- Andreozzi G.B., Bosi F. and Garramone F. (2001) - Synthetic spinels in the (Mg, Fe<sup>2+</sup>, Zn)(Al, Fe<sup>3+</sup>)<sub>2</sub>O<sub>4</sub> system: II. Preliminary chemical and structural data of hercynite and magnesioferrite samples. *Periodico di Mineralogia*, 70, 193-204.
- Basso R., Comin-Chiaramonti P., Della Giusta A. and Flora O. (1984) - Crystal chemistry of four Mg-Fe-Al-Cr spinels from the Balmuccia peridotite (Western Italian Alps). *Neues Jahrbuch für Mineralogie Abhandlungen*, 150, 1-10.
- Bosi F., Hålenius U. and Skogby H. (2009) - Crystal chemistry of the magnetite-ulvöspinel series. *American Mineralogist*, 94, 181-189.
- Comin-Chiaramonti P., Demarchi G., Sinigoi S. and Siena F. (1982) - Relazioni tra fusione e deformazione nella peridotite di Balmuccia (Ivrea-Verbanò). *Rendiconti della Società Italiana di Mineralogia e Petrologia*, 38, 685-700.
- Della Giusta A., Carbonin S. and Ottonello G. (1996) - Temperature-dependent disorder in a natural Mg-Al-Fe<sup>2+</sup>-Fe<sup>3+</sup>-spinel. *Mineralogical Magazine*, 60, 603-616.
- Della Giusta A., Princivalle F. and Carbonin S. (1987) - Crystal structure and cation distribution in some natural magnetites. *Mineralogy and Petrology*, 37, 315-321.
- Fujino K. (1974) - Cation distribution and local variation of site symmetry in solid solution series, Fe<sub>3</sub>O<sub>4</sub>-Fe<sub>2</sub>TiO<sub>4</sub>. *Mineralogical Journal*, 7, 472-488.
- Hamde H.H., Barghout K., Ho J.C., Shand P.M., and Miller L.L. (1999) - A Mössbauer evaluation of cation distribution in titanomagnetites. *Journal of Magnetism and Magnetic Materials*, 191, 72-78.
- Lavina B., Salviulo G. and Della Giusta A. (2002) - Cation distribution and structure modeling of spinel solid solutions. *Physics and Chemistry of Minerals*, 29, 10-18.
- Lenaz D., Piani E., Garuti G., Zaccarini F. and Princivalle F. (2005) - Crystalchemistry of chromite from the chromitites of the Finero mantle massif (Western Alps). (Abs.) *5<sup>th</sup> FIST Congress*.
- Lenaz D., Skogby H., Princivalle F. and Hålenius U. (2004) - Structural changes and valence states in the MgCr<sub>2</sub>O<sub>4</sub> - FeCr<sub>2</sub>O<sub>4</sub> solid solution series. *Physics and Chemistry of Minerals*, 31, 633-642.
- Lenaz D., Skogby H., Princivalle F. and Hålenius U. (2006) - The MgCr<sub>2</sub>O<sub>4</sub> - MgFe<sub>2</sub>O<sub>4</sub> solid solution series: effects of octahedrally coordinated Fe<sup>3+</sup> on T-O bond length. *Physics and Chemistry of Minerals*, 33, 465-474.
- Lindsley D.H. (1965) - Iron-titanium oxides. *Carnegie Inst. Washington Year Book*, 64, 144-148.
- Mehnert K.A. (1975) - The Ivrea Zone. A model of the deep crust. *Neues Jahrbuch für Mineralogie Abhandlungen*, 125, 156-199.
- Mukasa S.B. and Shervais J.W. (1999) - Growth of subcontinental lithosphere: evidence from repeated dyke injections in the Balmuccia lherzolite massif, Italian Alps. *Lithos*, 48, 287-316.
- North A.C.T., Phillips D.C. and Scott-Mattews F. (1968) - A semi-empirical method of absorption correction. *Acta Crystallographica*, A24, 351-352.

- Pearce C.I., Henderson C.M.B., Telling, N.D., Patrick R.A.D., Charnock J.M., Coker V.S., Arenholz E., Tuna F., and van der Laan G. (2010) - Fe site occupancy in magnetite-ulvöspinel solid solutions: a new approach using X-ray magnetic circular dichroism. *American Mineralogist*, 95, 425-439.
- Prince E. (2004) - International Tables for X-ray Crystallography. Volume C: Mathematical, Physical and Chemical Tables. 3<sup>rd</sup> edn. Springer, Dordrecht.
- Princivalle F., Della Giusta A. and Carbonin S. (1989) - Comparative crystal chemistry of spinels from some suits of ultramafic rocks. *Mineralogy and Petrology*, 40, 117-126.
- Rivalenti G., Mazzucchelli M., Vannucci R., Hofmann A.W., Ottolini L., Bottazzi P. and Obermiller W. (1995) - The relationship between websterite and peridotite in the Balmuccia peridotite massif (NW Italy) as revealed by trace element variations in clinopyroxene. *Contributions to Mineralogy and Petrology*, 121, 275-288.
- Shannon R.D. (1976) - Revised effective ionic radii and systematic studies of interatomic distances in halides and chalcogenides. *Acta Crystallographica*, A, 32, 751-767.
- Sheldrick G.M. (1997) - SHELX-97. Program for crystal structure refinement. University of Gottingen, Germany.
- Shervais J. (1979a) - Ultramafic and mafic layers in the alpine-type lherzolite massif at Balmuccia (Italy). *Memorie della Società Geologica di Padova*, 33, 135-145.
- Shervais J. (1979b) - Thermal emplacement model for the alpine lherzolite massif at Balmuccia (Italy). *Journal of Petrology*, 20, 795-820.
- Sinigoï S., Comin-Chiaramonti P., Demarchi G. and Siena F. (1983) - Differentiation of partial melts in the mantle: evidence from the Balmuccia peridotite, Italy. *Contributions to Mineralogy and Petrology*, 82, 351-359.
- Stout M.Z. and Bayliss P. (1975) - Crystal structure of a natural titanomagnetite. *Canadian Mineralogist*, 13, 86-88.
- Stout M.Z. and Bayliss P. (1980) - Crystal structure of two ferrian ulvöspinel from British Columbia. *Canadian Mineralogist*, 18, 339-341.
- Syono Y. (1965) - Magnetocrystalline anisotropy and magnetostriction of  $\text{Fe}_3\text{O}_4\text{-Fe}_2\text{TiO}_4$  series – with special application to rock magnetism. *Japanese Journal of Geophysics*, 4, 71-143.
- Tokonami M. (1965) - Atomic scattering factor for  $\text{O}^{2-}$ . *Acta Crystallographica*, 19, 486.
- Wechsler B.A., Lindsley D.H. and Prewitt C.T. (1984) - Crystal structure and cation distribution in titanomagnetites ( $\text{Fe}_{3-x}\text{Ti}_x\text{O}_4$ ). *American Mineralogist*, 69, 754-770.

Submitted, October 2010 - Accepted, January 2011